Inorg. Chem. **2007**, *46*, 3541–3547

Organic–Inorganic Hybrids Constructed of Anderson-Type Polyoxoanions and Oxalato-Bridged Dinuclear Copper Complexes

Ruige Cao, Shuxia Liu,* Linhua Xie, Yibing Pan, Jianfang Cao, Yuanhang Ren, and Lin Xu*

Key Laboratory of Polyoxometalates Science of Ministry of Education, College of Chemistry, Northeast Normal University, Changchun City, Jilin, PR China 130024

Received November 20, 2006

Two novel organic–inorganic hybrid compounds based on Anderson-type polyoxoanions, $[Cu_2(bpy)_2(\mu\text{-ox})][Al(OH)_7Mo_6O_{17}]$ (**1**) and $[Cu_2(bpy)_2(\mu\text{-ox})][Cr(OH)_7Mo_6O_{17}]$ (**2**), have been synthesized and characterized by elemental analyses, IR, and X-ray powder diffraction. The crystal structures of **1** and **2** have been established by single-crystal X-ray diffraction, which reveals the presence of 1D chains constructed of alternating Anderson-type polyoxoanions and oxalato-bridged dinuclear copper complexes for both compounds and extensive hydrogen bonding that plays an important role in the formation of the 3D supramolecular network structures of **1** and **2**. To elucidate the electronic properties and magnetic properties of the metal ions (Cu^{2+} or Cu^{2+} and Cr^{3+}), EPR studies and magnetic susceptibility studies have been performed, respectively. The results are consistent with the structural feature of these compounds.

Introduction

The rational design and synthesis of organic−inorganic hybrid materials possessing unique architectures and cooperative functional properties has been attracting considerable attention,[1] and so far, many organic−inorganic hybrid compounds have been reported.[2]

It is noteworthy that the polyoxoanions of polyoxometalates (POMs) have been extensively employed as inorganic building blocks for the construction of fancy 1D, 2D, and 3D organic−inorganic hybrid materials.[3] The evolution not only rests with variability of charges, shapes, and sizes at the molecular level for the polyoxoanions but also lies in their intriguing topologies and the wide range of potential applications in catalysis, medicine, electrical conductive, and magnetic materials.[4] To date, a number of hybrid materials constructed of well-defined polyoxoanions, such as Keggin,[5] Wells−Dawson,[6] and Lindquist[7] types, have been reported. In contrast, the use of Anderson-type polyoxoanions as inorganic building blocks in this aspect has not been widely explored.[8] It is well known that the Anderson-type polyoxoanions exhibit attractive planar structures. In addition,

* To whom correspondence should be addressed. E-mail: liusx@nenu.edu.cn (S.L.), linxu@nenu.edu.cn (L.X.). Fax: +86-431-85099328.

(1) (a) Carlucci, L.; Ciani, G.; Proserpio, D. M. *Coord. Chem. Rev.* **2003**, *246*, 247. (b) Moulton, B.; Zaworotko, M. J. *Chem. Rev.* **2001**, *101*, 1629. (c) Müller, A.; Reuter, H.; Dillinger, S. *Angew. Chem., Int. Ed. Engl.* **1995**, *34*, 2328. (d) Hagrman, P. J.; Hagrman, D.; Zubieta, J. *Angew. Chem., Int. Ed.* **1999**, *38*, 2638. (e) Kitaura, R.; Kitagawa, R. S.; Kubota, Y.; Kobayashi, T. C.; Kindo, K.; Mita, Y.; Matsuo, A.; Kobayashi, M.; Chang, H. C.; Ozawa, T. C.; Suzuki, M.; Sakata, M.; Takata, M. *Science* **2002**, *298*, 2358.

(2) (a) Zaworotko, M. J. *Angew. Chem., Int. Ed.* **1998**, *37*, 1211. (b) Lü, J.; Shen, E. H.; Yuan, M.; Li, Y. G.; Wang, E. B.; Hu, C. W.; Xu, L.; Peng, J. *Inorg. Chem.* **2003**, *42*, 6956. (c) Hong, C. S.; Do. Y. *Inorg. Chem.* **1998**, *37*, 4470. (d) Tao, J.; Zhang, X. M.; Tong, M. L.; Chen, X. M. *J. Chem. Soc., Dalton Trans.* **2001**, 770.

(3) (a) Wang, J. P.; Zhao, J. W.; Duan, X. Y.; Niu, J. Y. *Cryst. Growth Des.* **2006**, *6*, 507. (b) Wang, J. P.; Duan, X. Y.; Du, X. D.; Niu, J. Y. *Cryst. Growth Des.* **2006**, *6*, 2266. (c) Liu, S. X.; Xie, L. H.; Gao, B.; Zhang, C. D.; Sun, C. Y.; Li, D. H.; Su, Z. M. *Chem. Commun.* **2005**, 5023.

(4) (a) Pope, M. T. *Heteropoly and Isopoly Oxometalates;* Springer-Verlag: Berlin, 1983. (b) Hill, C. L.; Guest, Ed. Topical, Issue on Polyoxometalates. *Chem. Rev.* **1998**, *98*, 1−389. (c) *Polyoxometalates: From Platonic Solids to Anti-Retroviral Activity;* Pope, M. T., Müller, A., Eds.; Kluwer: Dordrecht, The Netherlands, 1993. (d) Hill, C. L. Polyoxometalates: Reactivity. In *Comprehensive, Coordination, Chemistry, II;* Wedd, A. G., Ed.; Elsevier, Science: New, York; Vol. 20044, pp 679−759. (e) Pope, M. T.; Müller, A. *Angew. Chem., Int. Ed. Engl.* **1991**, *30*, 34.

(5) (a) Zheng, P. Q.; Ren, Y. P.; Long, L. S.; Huang, R. B.; Zheng, L. S. *Inorg. Chem.* **2005**, *44*, 1190. (b) Ren, Y. P.; Kong, X. J.; Long, L. S.; Huang, R. B.; Zheng, L. S. *Cryst. Growth Des.* **2006**, *6*, 572. (c) Ren, Y. P.; Kong, X. J.; Hu, X. Y.; Sun, M.; Long, L. S.; Huang, R. B.; Zheng, L. S. *Inorg. Chem.* **2006**, *45*, 4016.

(6) (a) Bareyt, S.; Piligkos, S.; Hasenknopf, B.; Gouzerh, P.; Lacôte, E.; Thorimbert, S.; Malacria, M. *J. Am. Chem. Soc.* **2005**, *127*, 6788. (b) Niu, J. Y.; Guo, D. J.; Wang, J. P.; Zhao, J. W. *Cryst. Growth Des.* **2004**, *4*, 241.

(7) (a) Du, Y.; Rheingold, A. L.; Maatta, E. A. *J. Am. Chem. Soc.* **1992**, *114*, 345. (b) Wei, Y. G.; Lu, M.; Cheung, C. F. C.; Barnes, C. L.; Peng, Z. H. *Inorg. Chem.* **2001**, *40*, 5489. (c) Strong, J. B.; Ostrander, R.; Rheingold, A. L.; Maatta, E. A. *J. Am. Chem. Soc.* **1994**, *116*, 3601.

10.1021/ic062208c CCC: $37.00
Published on Web 04/05/2007

each Mo (or W) atom has two terminal oxygen atoms with high reactivity,[9] which may facilitate the construction of novel hybrid compounds.

On the other hand, a number of dinuclear copper complexes with oxalate bridging ligands have been largely structurally characterized and magnetically studied in the coordination chemistry field in the past few years,[10] because the oxalate group has shown to be an excellent bridging ligand to mediate magnetic exchange interactions between metal ions that are even far away from each other.[11] Recently, some hybrid compounds, which are assembled by polyoxoanions and oxalato-bridged dinuclear copper complexes, have been reported to display interesting magnetic properties, but the polyoxoanions are limited in monosubstituted Keggin-type $[SiW_{11}O_{39}Cu(H_2O)]^{6-}$ only.[12] Therefore, it will be of great impetus to research whether the oxalato-bridged dinuclear copper complex can interact with other types of polyoxoanions to obtain novel hybrid compounds. We isolated two novel organic−inorganic hybrid compounds, namely $[Cu_2(bpy)_2(\mu\text{-ox})][Al(OH)_7Mo_6O_{17}]$ (**1**) and $[Cu_2(bpy)_2(\mu\text{-ox})][Cr(OH)_7Mo_6O_{17}]$ (**2**), which are constructed of 1D chains of the Anderson-type polyoxoanions and the dinuclear copper complexes with oxalate bridging. The compounds represent the first successful example of integrating oxalato-bridged dinuclear copper complexes and Anderson-type polyoxoanions. Herein, the syntheses, structures, EPR, and magnetic property studies for the compounds have been reported.

Experimental Section

Materials and Methods. All of the reagents and solvents were purchased from commercial sources and used as received without further purification. Elemental analyses (C, H, and N) were performed on a Perkin-Elmer 2400 CHN elemental analyzer. Cr, Al, Cu, and Mo were determined by a Plasma-Spec(I) ICP atomic emission spectrometer. IR spectra were recorded in the range of 400−4000 cm^{-1} on an Alpha Centaurt FTIR spectrophotometer using KBr pellets. Powder X-ray diffraction measurements were performed on a Rigaku D/MAX-3 instrument with Cu Kα radiation in the angular range of $2\theta = 3-50°$ at 293 K. The electron paramagnetic resonance (EPR) spectra (X-band) were recorded on a Japanese JES-FE3AX spectrometer at room temperature (290 K) and liquid-nitrogen temperature (77 K), respectively. Magnetic susceptibility data were collected over the temperature range 300−2 K at a magnetic field of 1000 Oe for **1** and 5000 Oe for **2** on a Quantum Design MPMS-5 SQUID magnetometer.

Synthesis of $[Cu_2(bpy)_2(\mu\text{-ox})][Al(OH)_7Mo_6O_{17}]$ (1). Both the complex $[Cu_2(bpy)_2(\mu\text{-ox})]^{2+}$ (**A**) and the Anderson-type anion $[Al(OH)_7Mo_6O_{17}]^{2-}$ (**B**) were prepared in situ.[8a,b,12] In a typical synthesis procedure for **A**, a 10 mL methanol solution of 2,2′-bipyridine (0.093 g, 0.6 mmol) and a 10 mL aqueous solution of oxalic acid (0.0375 g, 0.3 mmol) were added dropwise to a 20 mL aqueous solution of $CuCl_2 \cdot 2H_2O$ (0.102 g, 0.6 mmol). For **B**, 0.9 g (3.72 mmol) of $Na_2MoO_4 \cdot 2H_2O$ was dissolved in 30 mL of water followed by the addition of 5 mL of glacial acetic acid and 10 mL of an aqueous solution containing 0.36 g of $AlCl_3 \cdot 6H_2O$ (1.5 mmol) with stirring. The pH of the solution was adjusted to 2.6 with a dilute HCl solution (3M). The solution of **A** was quickly added to that of **B** with stirring. A blue precipitate formed, and the resulting solution pH remained at 2.6 and was stirred for a while. The mixture was filtered; the filtrate was allowed to evaporate at room temperature. The blue block crystals of **1** were obtained within 4 days in about 68% yield (0.641 g, based on Mo). Anal. Calcd for $C_{22}H_{23}AlCu_2Mo_6N_4O_{28}$: C, 17.37; H, 1.52; N, 3.68; Al, 1.77; Cu, 8.36; Mo, 37.84. Found: C, 17.17; H, 1.35; N, 3.51; Al, 1.63; Cu, 8.43; Mo, 37.69. IR (KBr, cm^{-1}): 3446 (br), 1646 (s), 1626 (m), 1570 (m), 1496 (w), 1471 (m), 1445 (m), 1344 (m), 1313 (m), 1251 (w), 1164 (w), 1105 (m), 948 (m), 918 (s), 771 (m), 733 (m), 660 (s), 598 (m), 468 (m), and 435 (m).

Synthesis of $[Cu_2(bpy)_2(\mu\text{-ox})][Cr(OH)_7Mo_6O_{17}]$ (2). The synthesis of the complex $[Cu_2(bpy)_2(\mu\text{-ox})]^{2+}$ (**A**) of **2** was prepared following the procedure described above. For the Anderson-type polyoxoanion $[Cr(OH)_7Mo_6O_{17}]^{2-13}$ (**C**), 0.9 g (3.72 mmol) of $Na_2MoO_4 \cdot 2H_2O$ was dissolved in 30 mL of water, and the pH of the solution was carefully adjusted with a dilute HCl solution (3M) to approximately 4.5. Then a solution of $CrCl_3 \cdot 6H_2O$ (0.3 g, 1.12 mmol) in water (10 mL) was added. The solution of **A** was added into that of **C** with stirring. Immediately, blue precipitate formed, and the resulting solution pH was about 2.6. The mixture was stirred for 30 min and then filtered. The filtrate was kept for 5 days at ambient conditions, and blue block crystals of **2** were isolated in about 54% yield (0.518 g, based on Mo). Anal. Calcd for $C_{22}H_{23}CrCu_2Mo_6N_4O_{28}$: C, 17.09; H, 1.50; N, 3.63; Cr, 3.36; Cu, 8.22; Mo, 37.23. Found: C, 16.96; H, 1.43; N, 3.48; Cr, 3.48; Cu, 8.10; Mo, 37.35. IR (KBr, cm^{-1}): 3430 (br), 1645 (s), 1626 (m), 1565 (m), 1496 (w), 1445 (m), 1334 (m), 1312 (m), 1251 (w), 1164 (w), 1099 (w), 1035 (w), 949 (m), 920 (s), 769 (m), 728 (m), 655 (s), 587 (m), 475 (m), and 407 (m).

X-ray Crystallography. The reflection intensities of **1** and **2** were collected on a SMART CCD diffractometer equipped with graphite monochromatic Mo Kα radiation ($\lambda = 0.71073$ Å) at 293 K. The linear absorption coefficients, scattering factors for the atoms, and anomalous dispersion corrections were taken from *International Tables for X-ray Crystallography*. The structures were solved by the direct method and refined by the full-matrix least-squares method on F^2 using the SHELXTL crystallographic

(8) (a) Shivaiah, V.; Nagaraju, M.; Das, S. K. *Inorg. Chem.* **2003**, *42*, 6604. (b) Shivaiah, V.; Das, S. K. *Inorg. Chem.* **2005**, *44*, 8846. (c) An, H. Y.; Li, Y. G.; Wang, E. B.; Xiao, D. R.; Sun, C. Y.; Xu, L. *Inorg. Chem.* **2005**, *44*, 6062. (d) An, H. Y.; Li, Y. G.; Xiao, D. R.; Wang, E. B.; Sun, C. Y. *Cryst. Growth Des.* **2006**, *6*, 1107. (e) An, H.; Xiao, D.; Wang, E. B.; Li, Y. G.; Xu, L. *New J. Chem.* **2005**, *29*, 667.

(9) (a) Shivaiah, V.; Reddy, P. V. N.; Cronin, L.; Das, S. K. *J. Chem. Soc., Dalton Trans.* **2002**, 3781. (b) Drewes, D.; Limanski, E. M.; Krebs, B. *J. Chem. Soc., Dalton Trans.* **2004**, 2087. (c) Drewes, D.; Limanski, E. M.; Krebs, B. *Eur. J. Inorg. Chem.* **2004**, *4849*. (d) Gao, B.; Liu, S. X.; Xie, L. H.; Yu, M.; Zhang, C. D.; Sun, C. Y.; Cheng, H. Y. *J. Solid State Chem.* **2006**, *179*, 1681. (e) An, H. Y.; Xiao, D. R.; Wang, E. B.; Sun, C. Y.; Xu, L. *Eur. J. Inorg. Chem.* **2005**, *854*.

(10) (a) Felthouse, T. R.; Laskowski, E. J.; Hendrickson, D. N. *Inorg. Chem.* **1977**, *16*, 1077. (b) Julve, M.; Verdaguer, M.; Gleizes, A.; Philoche-Levisalles, M.; Kahn, O. *Inorg. Chem.* **1984**, *23*, 3808. (c) Julve, M.; Faus, J.; Verdaguer, M.; Gleizes, A. *J. Am. Chem. Soc.* **1984**, *106*, 8306.

(11) (a) Coronado, E.; Galán-Mascarós, J. R.; Gómez-García, C. J.; Laukhin, V. *Nature* **2000**, *408*, 447. (b) Li, L. L.; Lin, K. J.; Ho, C. J.; Sun, C. P.; Yang, H. D. *Chem. Commun.* **2006**, 1286. (c) Kurmoo, M.; Graham, A. W.; Day, P.; Coles, S. J.; Hursthouse, M. B.; Caulfield, J. L.; Singleton, J.; Pratt, F. L.; Hayes, W.; Ducasse, L.; Guionneau, P. *J. Am. Chem. Soc.* **1995**, *117*, 12209.

(12) (a) Reinoso, S.; Vitoria, P.; Lezama, L.; Luque, A.; Gutiérrez-Zorrilla, J. M. *Inorg. Chem.* **2003**, *42*, 3709. (b) Reinoso, S.; Vitoria, P.; Gutiérrez-Zorrilla, J. M.; Lezama, L.; San Felices, L.; Beitia, J. I. *Inorg. Chem.* **2005**, *44*, 9731.

(13) Perloff, A. *Inorg. Chem.* **1970**, *9*, 2228.

Table 1. Crystal Data and Structural Refinements for **1** and **2**

compounds	**1**	**2**
empirical formula	$C_{22}H_{23}AlCu_2Mo_6N_4O_{28}$	$C_{22}H_{23}CrCu_2Mo_6N_4O_{28}$
M	1521.14	1546.16
T (K)	293(2)	293(2)
wavelength (Å)	0.71073	0.71073
cryst syst	orthorhombic	orthorhombic
space group	*Pna*2(1)	*Pna*2(1)
a (Å)	14.2454(8)	14.2385(7)
b (Å)	26.2933(14)	26.3312(13)
c (Å)	10.2411(5)	10.2825(5)
V (Å^3)	3835.9(4)	3855.1(3)
Z	4	4
D_c (mg/m^3)	2.634	2.664
abs coeff (mm^{-1})	3.112	3.341
reflns collected	19 883	19 912
independent reflns	6149	6772
θ range (deg)	1.55−25.60	1.55−25.59
GOF on F^2	1.033	1.024
R_1 ($I > 2\sigma(I)$)[a]	0.0346	0.0416
wR_2 (all data)[b]	0.0686	0.0831

[a] $R_1 = \sum||F_o| - |F_c||/\sum|F_o|$. [b] $wR_2 = [\sum w(F_o^2 - F_c^2)^2/\sum w(F_o^2)^2]^{1/2}$.

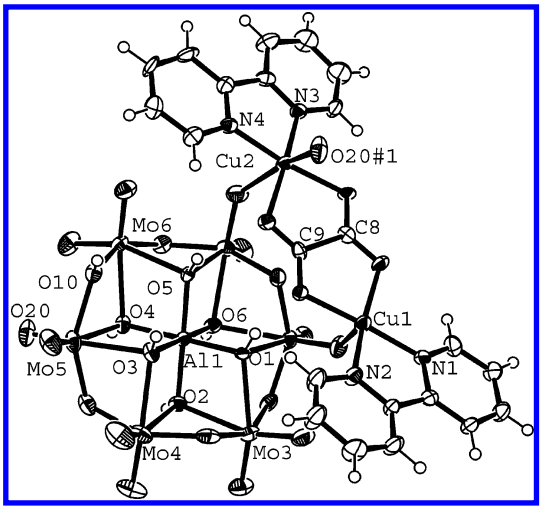

Figure 1. ORTEP view of **1** with thermal ellipsoids at 50% level. Only partial atoms are labeled for clarity. Symmetry transformations used to generate equivalent atoms: #1 $x, y, z - 1$.

software package. Anisotropic thermal parameters were used to refine all non-hydrogen atoms. Hydrogen atoms on the 2,2′-bipyridine ligands were placed on calculated positions and included in the refinement riding on their respective parent atoms. All of the hydrogen atoms for protonation were located in the difference Fourier maps, and their positions were refined using isotropic thermal parameters. The crystal data and structure refinement results of **1** and **2** are summarized in Table 1. Selected bond lengths and bond angles for **1** and **2** are provided in Tables S1 and S2 in the Supporting Information. The experimental and simulated X-ray powder diffraction patterns (XRPD) of both compounds are shown in Figure S5. The diffraction peaks on both experimental and simulated patterns match well in position, indicating their phase purity. Additionally, the XRPD of **1** and **2** are similar, which is in agreement with their isomorphic structures determined by single-crystal X-ray diffraction.

Results and Discussion

Synthesis. 1 and **2** were synthesized from the solution reaction of $[Cu_2(bpy)_2(\mu\text{-ox})]^{2+}$ and the Anderson-type polyoxoanions, which were both prepared in situ. The differences in the reaction conditions for the two compounds, such as the length of stirring time and the presence or absence of glacial acetic acid, may rely on the intrinsic character of the polyoxoanions. After plenty of parallel experiments, it was found that adjustment of the pH of the mixture to 2.6 is crucial for the syntheses of **1** and **2**.

Crystal Structures. 1 $[Cu_2(bpy)_2(\mu\text{-ox})][Al(OH)_7Mo_6O_{17}]$ and **2** $[Cu_2(bpy)_2(\mu\text{-ox})][Cr(OH)_7Mo_6O_{17}]$ are isomorphic with similar unit-cell parameters, related bond lengths and bond angles, and **1** is described as an example below. The asymmetric unit of **1** contains one Anderson-type polyoxoanion $[Al(OH)_7Mo_6O_{17}]^{2-}$ and one oxalato-bridged dinuclear copper complex $[Cu_2(bpy)_2(\mu\text{-ox})]^{2+}$, as shown in Figure 1. Further studies reveal that **1** is constructed from 1D chains, which consist of alternating Anderson-type polyoxoanions and dinuclear copper complexes, running along the c axis. (Figure 2) The building block $[Al(OH)_7Mo_6O_{17}]^{2-}$ belongs to B-type Anderson structure, which consists of seven edge-sharing octahedra, six of which are $[MoO_6]$ octahedral, arranged hexagonally around the central $[Al(OH)_6]$ octahedron. The difference Fourier maps indicate that six μ_3-bridging oxygen atoms (O1−O6) around the Al^{3+} ion and a μ_2-bridging oxygen atom (O10) are protonated. The Mo−O and the central Al−O bond lengths lie in the ranges of 1.698(5)−2.353(5) and 1.879(6)−1.921(6) Å, respectively. The bond angles of $O-Al-O_{cis}$ range from 84.4(2) to 95.8(2)° and $O-Al-O_{trans}$ vary from 179.0(3) to 179.5(3)°. All of the bond lengths and bond angles are within the normal ranges and are consistent with those described in the literature.[8a,b]

The dinuclear copper complex with oxalate bridging in the usual bis-bidentate fashion is noncentrosymmetric. As can be seen in Figure 1, there are two independent copper centers in which Cu1 is five-coordinated in distorted square-pyramidal coordination geometry and Cu2 is six-coordinated in elongated octahedral coordination geometry, which are respectively completed by two oxalate oxygen atoms and two bipyridine nitrogen atoms at the equatorial sites and one or two terminal oxygen atoms from the Anderson-type polyoxoanions at the apical positions with a Cu1···Cu2 distance of 5.157(4) Å. Interestingly, the $Cu-O_t$ bond lengths are obviously different, ranging from 2.476(6) to 3.033(2) Å, so the complex might be regarded as weakly coordinated or even noncoordinated to terminal oxygen atoms as a result of the difference of copper coordination geometry. The geometry of a oxalato-bridged dinuclear copper complex is neither classic boat nor chair conformation;[14] the oxalate group and bpy ligands are non-coplanar. The oxalate group is nearly planar (largest deviation of atoms from the mean plane is 0.008(8) Å) with a long C−C bond length of 1.568(9) Å. The values of the dihedral angles between the mean plane and that of Cu1N1N2 and Cu2N3N4 are 18.3(7) and 13.1(2)°, respectively.

(14) Alvarez, S.; Julve, M.; Verdaguer, M. *Inorg. Chem.* **1990**, *29*, 4500.

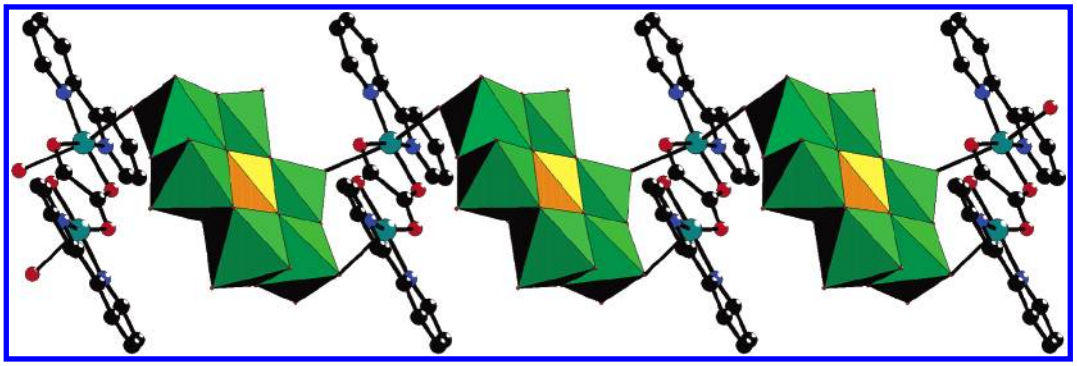

Figure 2. Polyhedral representation of the 1D chain running along the *c* axis of **1**. All of the hydrogen atoms have been omitted for clarity. Color code: Al, light orange; Mo, green; Cu, teal; N, blue; C, black; O, red.

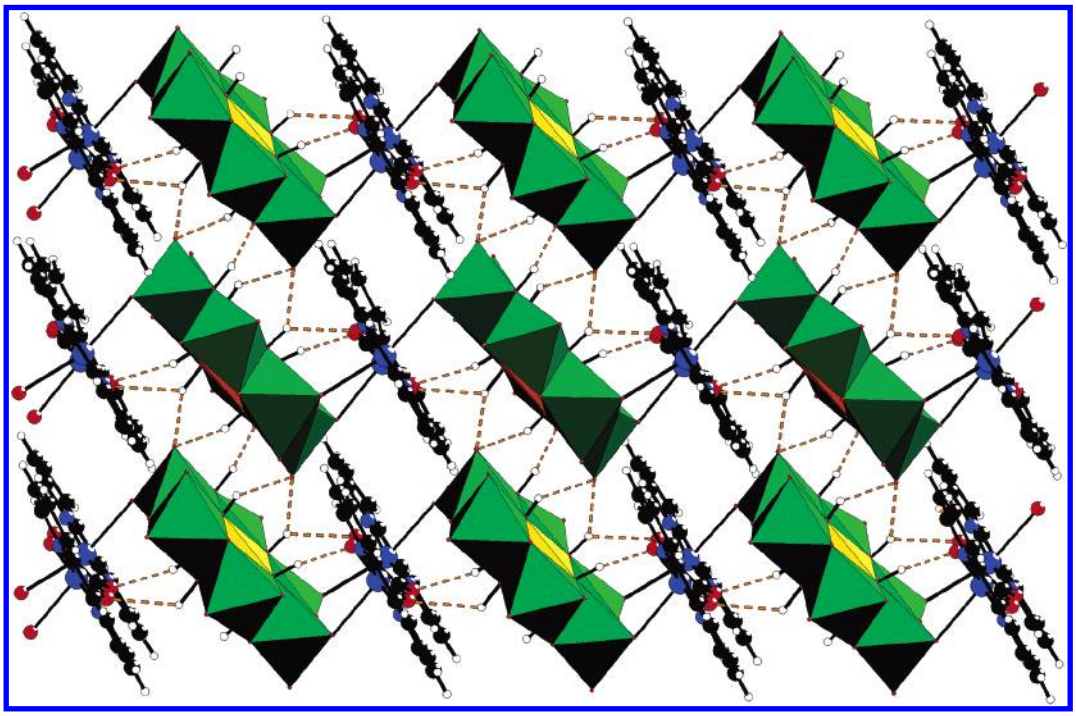

Figure 3. Intrachain and interchain hydrogen bonds in **1**. Color code: Al, light orange; Mo, green; Cu, teal; N, blue; C, black; O, red.

It is striking that the structure of **1** exhibits three types of hydrogen bonds. The first type is intrachain hydrogen bonds between the protonated oxygen atoms (donors) in $AlMo_6$ polyoxoanions and the oxalate oxygen atoms (acceptors) within the same chain. The second interchain hydrogen bonds occur between the protonated oxygen atoms and the terminal oxygen atoms in neighboring chains, which contribute to the formation of the 2D layer parallel to the *ac* plane. (Figure 3) Finally, interlayer C−H(bpy)···O_t interactions lead to the 3D supramolecular network structure (Figure S1). The typical hydrogen bond parameters are listed in Table 2. It is believed that the extensive hydrogen bonding interactions play an important role in the construction of structure **1**.

The bond-valence calculations suggest that Al and Cr atoms are in the +3 oxidation state, all Cu atoms are in the +2 oxidation state, and all Mo atoms are in the +6 oxidation state in **1** and **2**. Bond-valence calculations for all of the oxygen atoms confirmed the results of X-ray single-crystal diffraction determination that there are seven oxygen atoms protonated, respectively.

IR Spectroscopy. The IR spectra of **1** and **2** are alike (Figure S3). In the low-wavenumber regions of the IR spectra, they display similar characteristic patterns of the Anderson-type structure,[8] with vibrational bands between 890 and 950 cm^{-1} for the Mo−O_t bonds, between 660 and 740 cm^{-1} for the Mo−O_b groups, and between 400 and 600 cm^{-1} for the Mo−O_c units. The characteristic peaks that range from 1100 to 1600 cm^{-1} are attributed to the 2,2′-bipyridine ligand, which are of low intensity with respect to those of the Anderson-type polyoxoanions. The features at about 775 cm^{-1} are assignable to ν_{as}(CO), those at 1313 and 1344 cm^{-1} are assigned to ν_s(CO), and the broad absorption at 1646 cm^{-1} corresponds to ν(OCO) of the oxalate ligand in a bis-bidentate bridging mode.[15]

EPR Spectroscopy. The X-band powder EPR spectra of **1** and **2** were recorded at room temperature and liquid nitrogen temperature, respectively, as shown in Figure 4. For

(15) (a) Tuero, L. S.; Garcia-lozano, J.; Monto, E. E.; Borja, M. B.; Dahan, F.; Tuchagues, J. P.; Legros, J. P. *J. Chem. Soc., Dalton Trans.* **1991**, 2619. (b) Thomas, A. M.; Mandal, G. C.; Tiwary, S. K.; Rath, R. K.; Chakravarty, A. R. *J. Chem. Soc., Dalton Trans.* **2000**, 1395.

Table 2. Geometrical Parameters of Hydrogen Bonds (anstroms, deg) in **1**[a]

	D−H···A[b]	*d*(D−H)	*d*(H···A)	*d*(D···A)	∠DHA
intrachain	O(2)−H(23)···O(28)#1	0.924	2.510	3.251	137.49
	O(2)−H(23)···O(19)#2	0.924	2.185	2.973	142.72
	O(3)−H(24)···O(14)#3	0.938	2.029	2.834	142.81
intrachain	O(1)−H(25)···O(27)	0.971	1.951	2.876	158.14
	O(10)−H(26)···O(7)#3	1.084	1.535	2.604	167.63
	O(5)−H(27)···O(14)#3	0.878	2.273	2.915	129.86
intrachain	O(5)−H(27)···O(25)	0.878	2.364	3.081	139.01
intrachain	O(4)−H(28)···O(26)#1	0.827	2.176	2.941	153.93
	O(6)−H(29)···O(19)#2	0.830	2.212	2.873	136.74
	C(1)−H(1)···O(13)#3	0.930	2.472	3.206	135.80
	C(6)−H(6)···O(18)#4	0.932	2.563	3.271	133.01
	C(10)−H(10)···O(20)#2	0.931	2.318	3.025	132.39
	C(15)−H(15)···O(15)#5	0.931	2.568	3.166	122.35
	C(16)−H(16)···O(21)#6	0.931	2.333	3.203	155.46
	C(18)−H(18)···O(15)#5	0.930	2.541	3.155	123.92
	C(22)−H(22)···O(24)#3	0.929	2.433	3.052	124.07

[a] *D* = donor, *A* = acceptor. [b] Symmetry transformations used to generate equivalent atoms: #1 $x, y, z+1$; #2 $x-{}^1/_2, -y+{}^3/_2, z$; #3 $x+{}^1/_2, -y+{}^3/_2, z$; #4 $x-{}^1/_2, -y+{}^3/_2, z-1$; #5 $-x+1, -y+1, z-{}^1/_2$; #6 $-x+{}^3/_2, y-{}^1/_2, z-{}^1/_2$.

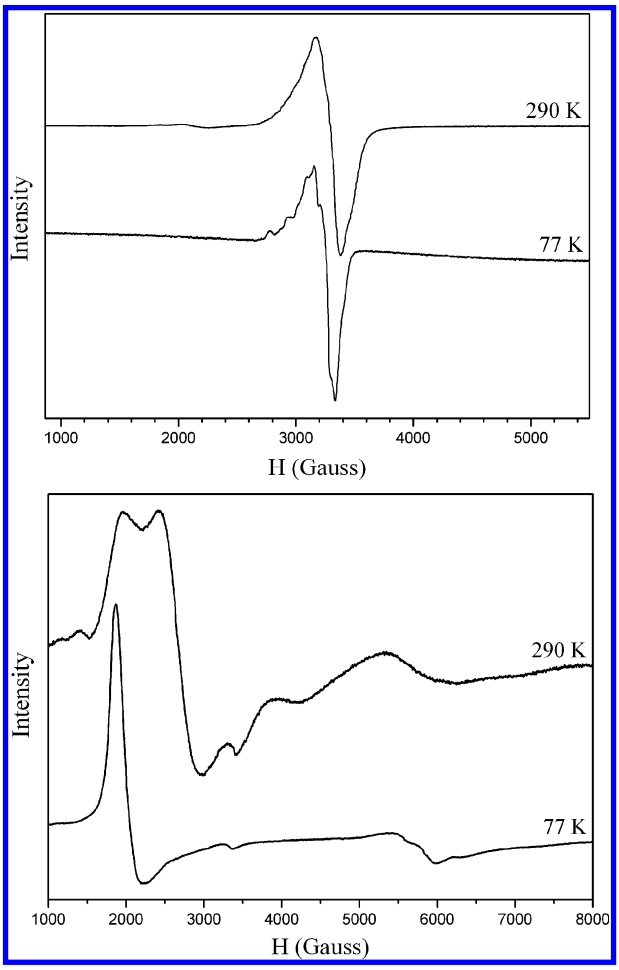

Figure 4. X-band EPR spectra of **1** (top) and **2** (bottom) at room temperature ($\nu = 9.4410$ GHz) and liquid-nitrogen temperature ($\nu = 9.2000$ GHz), respectively.

1, the two spectra consist of a broad signal centered at about 3200 G, as expected for copper(II) systems. At room temperature, a weak signal at low field around 2000 G is observed. The resolution in the parallel region of the spectrum is considerably improved when recorded at the liquid nitrogen temperature, which should be attributed to the signal narrowing induced by the increasing spin−lattice relaxation time. At the same time, the weak signal disappears. Moreover, at 77 K the values for $g_{\|}$ and $g_{\perp}$ are 2.239 and 2.027, respectively, and the high $g_{\|}$ value reveals a low Jahn−Teller effect associated with the octahedrally coordinated Cu^{2+} with the unpaired electron on the $d_{x^2-y^2}$ orbital.

The spectra of **2** are more complicated in comparison with those of **1** as a result of the presence of different paramagnetic resonance centers of Cr^{3+} and Cu^{2+} ions, (Figure 4). The coordination geometry around Cr^{3+} is distorted octahedral, which usually gives rise to the zero-field splitting.[16] In the spectrum at room temperature, the effective *g* values $g \approx 4.665$, 3.241, and 2.523 may attributed to the electronic spin $S = {}^3/_2$ for Cr^{3+} with large zero-field splitting. The weak broad high-field signals are also observed with a magnetic field corresponding to $g < 2$.[8d,17] It is noteworthy that there is a featureless resonance at the *g* value centered about $g \approx 1.995$, indicating that it possibly arises from the copper(II) systems.[8b] Furthermore, several smaller features are found at low field. Surprisingly, at 77 K the spectra changes a lot for Cr^{3+}, with signals centered at $g \approx 3.233$ (2030 G) and $g \approx 1.150$ (5720 G). However, the signal for copper(II) systems at $g \approx 1.981$ remains at around 3320 G compared to that of the spectrum at room temperature with a slight difference in the *g* value. It is worth reminding that the expected hyperfine structure of copper(II) systems at 77 K is likely to be masked by the relatively stronger intensity of the signal for Cr^{3+}. Such spectra are associated with relatively large zero-field splitting, which is consistent with literature data.[18]

Magnetic Properties. Thermal evolution of the magnetic molar susceptibility and the $\chi_m T$ product in the temperature

(16) (a) Jacquamet, L.; Sun, Y. J.; Hatfield, J.; Gu, W. W.; Cramer, S. P.; Crowder, M. W.; Lorigan, G. A.; Vincent, J. B.; Latour, J. M. *J. Am. Chem. Soc.* **2003**, *125*, 774. (b) Casellato, U.; Graziani, R.; Bonomo, R. P.; Di Bilio, A. J. *J. Chem. Soc., Dalton Trans.* **1991**, 23.
(17) Rojo, J. M.; Mesa, J. L.; Lezama, L.; Rojo, T. *J. Mater. Chem.* **1997**, *7*, 2243.
(18) (a) Chakradhar, R. P. S.; Murali, A.; Rao, J. L. *J. Alloys Comput.* **1998**, *281*, 99. (b) Golhen, S.; Ouahab, L.; Grandjean, D.; Molinié, P. *Inorg. Chem.* **1998**, *37*, 1499. (c) Pedersen, E.; Toftlund, H. *Inorg. Chem.* **1974**, *13*, 1603.

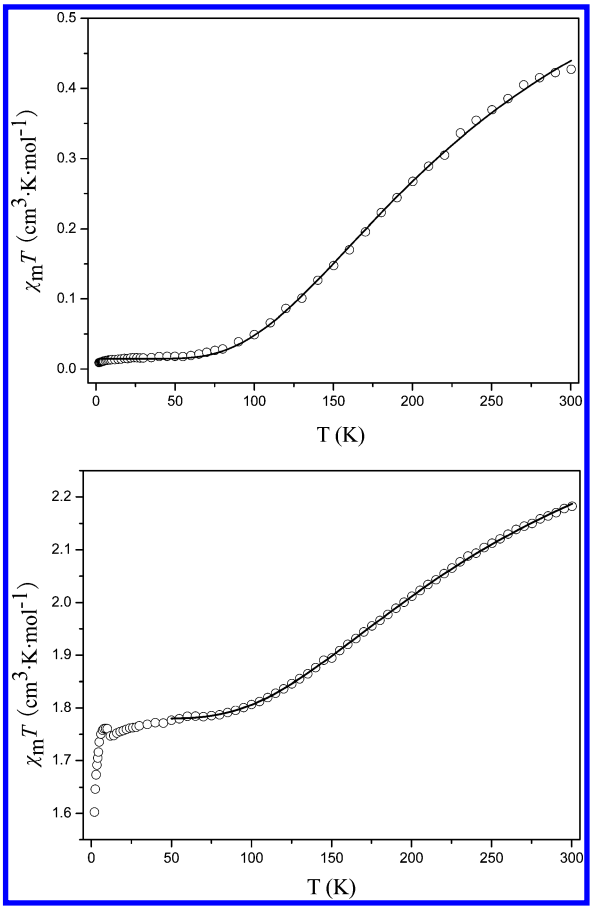

Figure 5. $\chi_m T$ curves of **1** (top) and **2** (bottom). Continuous lines display the results of the least-squares fit to eq 2.

range 300−2 K are shown in Figure S4 and Figure 5, respectively. As expected, while the structures of both compounds are similar, there are different magnetic curves because of the presence of the paramagnetic Cr^{3+} ion in **2**. At room temperature, $\chi_m T$ values (**1**, 0.427; **2**, 2.188 cm^3·K·mol^{-1}) are substantially lower than those values expected for the magnetically uncoupled centers with $\chi_m T = \mu_{eff}^2/8$ (**1**, 0.750; **2**, 2.625 cm^3·K·mol^{-1}, assuming $g = 2$). For **1**, the value of $\chi_m T$ continuously decreases as the temperature decreases from 300 to 55 K and remains constant around 0.015 cm^3·K·mol^{-1} below 55K, which is associated with the paramagnetic impurities. However, for **2**, upon cooling the samples, the value of $\chi_m T$ falls around 1.769 cm^3·K·mol^{-1} between 75 and 12 K, which is close to one uncoupled Cr^{3+} ion, and the $\chi_m T$ rapidly decreases below 2 K mostly because of the large zero-field splitting of $S = {}^3/_2$ spin of Cr^{3+} ion, which is in accord with the result of EPR.

The decrease in $\chi_m T$ is indicative of antiferromagnetic coupling in the oxalato-bridged dinuclear copper complexes, while the plateau corresponds to the Curie law expected for the paramagnetic impurities or the paramagnetic center Cr^{3+} ion, which dominates at low temperature with no detectable interactions between them.

The intramolecular exchange interactions can be represented by the isotropic spin Hamiltonian equation

$$\hat{H} = -J\hat{S}_A \cdot \hat{S}_B \qquad (1)$$

where J is the exchange integral and $S_A = S_B = {}^1/_2$. The χ_m may be expressed as eq 2 according to the Bleaney−Bowers equation for isotropic exchange in the copper (II) dimer.[19]

$$\chi_m = A\left[\frac{(1-\rho)Ng^2\beta^2}{kT[3+\exp(-J/kT)]} + \frac{\rho Ng^2\beta^2}{4kT}\right] + B\frac{5Ng'^2\beta^2}{4kT} \qquad (2)$$

This equation has been modified to take into account the admixture of paramagnetic impurities, where N, β, and k have their usual meanings, ρ is the fraction of noncoupled impurities, g is the g-factor of the dinuclear copper complex, and g' is the g-factor of the Cr^{3+} in the Anderson-type polyoxoanion. The A and B factors correspond to the number of Cu^{2+} and Cr^{3+} ions, respectively, with $A = 2$, $B = 0$ for **1** and $A = 2$, $B = 1$ for **2**. Because the Cr^{3+} ions display relatively large zero-field splitting, we fit the $\chi_m T$ curve range from only 300 to 50 K for **2**. Moreover, the paramagnetic contribution of Cr^{3+} ions may be large enough compared to the noncoupled impurities, therefore ρ was fixed to zero during the fitting procedure for **2**.

Least-square fits of eq 2 to the data were performed by minimizing eq 3, where NP is the number of data points and NV is the number of variable parameters.[12,20]

$$R = \{\sum_{i=1}^{NP}[\chi_m(\text{exptl})_i - \chi_m(\text{calcd})_i]^2/(NP - NV)\}^{1/2} \qquad (3)$$

The best fit results are $J = -315$ cm^{-1}, $g = 2.09$, $\rho = 1.8\%$, and $R = 1.0 \times 10^{-5}$ for **1** and $J = -332$ cm^{-1}, $g = 2.08$, $g' = 1.95$, and $R = 3.5 \times 10^{-6}$ for **2**. The observed J values of **1** and **2** are smaller than those previously reported compounds of coplanar orbital topology.[14]

Conclusions

In short, the oxalato-bridged dinuclear copper complexes have been introduced into the Anderson-type frameworks successfully, which formed two novel organic−inorganic hybrid compounds. EPR studies of **1** display a signal for copper(II) systems. However, for **2**, containing both Cr^{3+} and Cu^{2+} ions, the studies show large zero-field splitting of the Cr^{3+} ion, and a signal for the copper(II) systems. Magnetic susceptibility studies reveal the strong antiferromagnetic coupling in the dinuclear copper complexes with J values of -315 cm^{-1} for **1** and -332 cm^{-1} for **2**. The results of EPR and magnetic susceptibility studies are in agreement with the structural feature of these compounds.

This work reveals that the cationic oxalato-bridged dinuclear copper complexes were stable in solution and can be crystallized with Anderson-type polyanions. This fact implies that the oxalato-bridged dinuclear copper complexes may interact with many other types of polyoxoanions using similar procedures. It is hoped that a number of organic−inorganic hybrid compounds based on this system will be

(19) Wojciechowski, W. *Inorg. Chim. Acta* **1967**, *1*, 319.
(20) (a) San Felices, L.; Vitoria, P.; Gutiérrez-Zorrilla, J. M.; Reinoso, S.; Etxebarria, J.; Lezama, L. *Chem.—Eur. J.* **2004**, *10*, 5138. (b) Reinoso, S.; Vitoria, P.; San Felices, L.; Lezama, L.; Gutiérrez-Zorrilla, J. M. *Chem.—Eur. J.* **2005**, *11*, 1538.

isolated soon for further investigation. In fact, we have already synthesized a series of hybrid compounds built from rare earth ions, substituted polyoxoanions, and $[Cu_2(bpy)_2(\mu\text{-ox})]^{2+}$ complexes, which will be reported soon.

Acknowledgment. This work was supported by the National Science Foundation of China (grant no. 20571014) and the Scientific Research Foundation for Returned Overseas Chinese Scholars, the Ministry of Education.

Supporting Information Available: X-ray crystallographic data for **1** and **2** and additional figures and tables. This material is available free of charge via the Internet at http://pubs.acs.org.

IC062208C